Advances in Science and Technology Research Journal

Advances in Science and Technology Research Journal, 2025, 19(10), 396–411
https://doi.org/10.12913/22998624/208693
ISSN 2299-8624, License CC-BY 4.0

Received: 2025.07.16
Accepted: 2025.08.15
Published: 2025.09.01

Influence of graphene nanoplatelets on the interfacial bonding and mechanical performance of flax/epoxy composites

K. Y. Eayal Awwad[1*], Rasheed Abdullah[1,2], Mohammad Alhawamdeh[3], Raed Al-Rbaihat[1], Sameh Alsaqoor[1], Nabeel Alshabatat[1]

[1] Department of Mechanical Engineering, Faculty of Engineering, Tafila Technical University, Tafila 66110, Jordan
[2] Department of Architecture and Design, Al-Zaytoonah University of Jordan, Amman 11733, Jordan
[3] Department of Civil Engineering, School of Engineering, Tafila Technical University, Tafila 66110, Jordan
* Corresponding author's e-mail: k.awwad@ttu.edu.jo

ABSTRACT

The development of sustainable, high-performance composite materials has led to an increasing interest in natural fiber-reinforced polymers enhanced with nanofillers. This study investigates the effect of graphene nanoplatelets (GnPs) on the interfacial and mechanical properties of flax fiber-reinforced epoxy composites. The GnPs were added at concentrations ranging from 0 wt.% to 6 wt.% while maintaining a constant flax fiber volume fraction of 25%. The mechanical performance of Flax/Epoxy/GnPs (F/E/GnPs) composites was assessed alongside their corresponding Epoxy/GnPs (E/GnPs) matrix composites. The interlaminar shear strength (ILSS) of the F/E/GnPs composites was measured using the short-beam bending method. Results showed that the GnPs addition decreased the fracture strength, fracture strain, and toughness in the E/GnPs matrix composites but significantly improved the stiffness. Incorporating flax fiber into these matrix composites enhanced the mechanical strength across all compositions. Notably, the F/E/1.5GnPs composite demonstrated optimal performance, with a 166% increase in the fracture strength and a 500% increase in the modulus of elasticity compared to E/1.5GnPs, alongside an 18% improvement in ILSS relative to neat epoxy. These improvements were attributed to the better interfacial adhesion and stress transfer caused by the uniform GnPs dispersion. However, increasing the GnPs content beyond 1.5 wt.% led to agglomeration and higher matrix viscosity, which weakened the fiber wetting and reduced interfacial bonding. SEM analysis of E/GnPs matrix composites revealed a more brittle fracture behaviour with a higher GnPs content. In the F/E/GnPs composites, excessive GnPs content further reduced the interfacial cohesion between flax fibers and the epoxy resin, likely caused by limited wetting during the fabrication process. These findings highlight the importance of optimising the GnPs content to balance the strength, adhesion, and processability in natural fiber composites.

Keywords: epoxy composites; flax fiber; graphene nanoplatelets, interfacial strength.

INTRODUCTION

Recently, natural fibers have gained significant attention as potential reinforcements for polymers, serving as either full or partial replacements for synthetic fibers. Due to their availability, renewability, and relatively low cost, natural fibers have emerged as promising raw materials for bio-composites [1–3]. This growing interest is driven by the urgent need to reduce the environmental impact of synthetic materials and address challenges associated with their disposal and recycling [3–5]. However, natural fibers exhibit somewhat lower mechanical properties and weaker interfacial bonding strength with polymer matrices compared to synthetic fibers. These limitations stem primarily from their hydrophilic chemical composition and physical characteristics, which vary depending on factors such as climate, age, and retting processes [6, 7]. To address these challenges, researchers have developed various strategies, including chemical treatments, hybridization of synthetic and

natural fibers, and the incorporation of additives, to enhance the performance of polymer composites reinforced with natural fibers (NFRPs).

Fiber–matrix adhesion in fiber-reinforced polymer systems is critical in determining the overall performance of composite materials [8, 9]. Strong interfacial bonding enhances the ability of the matrix to transfer the applied loads directly to the embedded fibers, thereby enhancing the tensile strength, wear resistance, and fatigue life. Conversely, the poor interfacial adhesion can lead to stress concentrations, fiber pull-out, and premature failure under mechanical loading [9]. To address these challenges, extensive research has been conducted to evaluate techniques for improving interfacial bonding strength in natural fiber-reinforced polymer composites (NFRPCs). A widely adopted approach involves chemical treatments to modify the inherently hydrophilic nature of natural fibers, which exhibit poor adhesion to hydrophobic polymer matrices due to their hydroxyl- and carboxyl-rich composition [10, 11]. Consequently, surface modifications are necessary to enhance interfacial bonding and improve composite performance [10, 12]. In addition to chemical treatments, various physical treatment methods have also been explored to strengthen the fiber-matrix interface in NFRPCs, as reported in [13, 14]. The primary challenges that reported included the inconsistent geometry of the fibers, and the variation in fiber–matrix adhesion – even within individual fiber samples [15].

Both chemical and physical treatments have demonstrated the essential need for modifying natural fibers to enhance the overall performance of NFRPCs. Today, engineered natural fibers – chemically treated and modified – are readily available in stores and nearly ready for direct use. As a result, recent research has increasingly shifted its focus toward further modifications to enhance the bonding strength of NFRPCs. One such approach involves the use of additives, particularly nano-additives. Due to their nanoscale dimensions, these additives have garnered significant attention in the scientific community, driving research toward innovative solutions for future applications. With a higher aspect ratio than micro-additives, nanoparticles play a crucial role in polymeric composites by providing a significantly larger filler-specific surface area, thereby improving interfacial interactions and overall composite performance [9].

From In the literature, numerous studies have explored the effects of various nano-additives on the bonding strength between fibers and polymer resins. However, most of the published works focus on synthetic fiber-reinforced polymers, such as silica nanoparticles with carbon/epoxy composites [9, 16], graphene nanoplatelets (GnPs) with glass/epoxy composites [17], GnPs with carbon/epoxy composites [18, 19], and graphene oxide (GO) with carbon /epoxy composites [20, 21], among others. In the context of NFRPCs, Dang et al. [22] investigated the effect of GO on the interlaminar shear strength (ILSS) of ramie fiber/polypropylene composites. The study explored the effects of different weight contents and particle sizes, revealing that a medium grain size of 5 μm GO particles enhanced the ILSS by 32% compared to untreated ramie fiber/polypropylene composites, representing the optimal size and weight content of GO particles. Nevertheless, studies exploring the effects of nanofillers on the bonding strength of natural fibers and polymer resins remain limited. There is a clear need to investigate the effects of a wider range of nanofiller materials on the interfacial bonding strength between natural fibers and polymer resins.

In our previous studies, we investigated the mechanical and tribological properties of epoxy composites reinforced with different weight fractions (0–4.5 wt.%) of GnPs [23], as well as the combined effect of GnPs (0, 1.5, and 3 wt.%) and flax fiber (25 vol.%) as reported in [24]. The results demonstrated a positive synergistic effect of GnPs and flax fiber on both the mechanical and tribological properties of the epoxy matrix. The reported findings motivated the current work, which aims to explore the influence of GnPs on the ILSS between flax fibers and epoxy resin.

Building upon our previously published research [23, 24], this investigation prepared additional fabricated composites to explore more thoroughly how GnPs influence composite behaviour. The GnPs content is extended to a range of 0–6 wt.% while maintaining a constant flax fiber volume fraction of 25%. The effects of GnPs on the interfacial and mechanical properties of flax/epoxy composites are evaluated, including the ILSS, fracture strength, toughness, stiffness, and hardness. Characterisation analysis is conducted on the epoxy/GnPs (E/GnPs) matrix composites. The SEM is used to study the morphology and fracture surfaces. A detailed comparative analysis is performed between the flax/epoxy/GnPs (F/E/GnPs) composites and their corresponding E/GnPs base matrices to gain deeper insights into the fiber–matrix–nanoparticle interactions.

MATERIALS AND METHODS

Materials

In this study, a thermosetting polymer matrix was formulated using R246TX epoxy resin combined with H160 hardener in a 4:1 weight ratio, both sourced from ATL Composites Pty. Ltd., Australia. Grade C graphene nanoplatelets (GnPs) with a specific surface area of 300 m^2/g manufactured by Sigma-Aldrich Pty. were incorporated as the nanoscale filler in the composite system. The epoxy/GnPs matrix was reinforced using a unidirectional flax fabric (Lineo, Belgium), characterized by 0.36 mm thickness and 200 g/m^2 areal density.

Sample preparation

The composite fabrication process was executed in two sequential stages. Initially, epoxy/GnPs (E/xGnPs) matrix systems were developed using different GnPs loadings – namely 0, 1.5, 3, 4.5, and 6 wt.% – where "x" indicates the weight percentage. These specific concentrations were chosen to minimize the likelihood of nanoparticle agglomeration within the epoxy matrix and to control viscosity, as higher viscosity impedes the effective infusion of the E/xGnPs matrix composites through the fiber reinforcement. Furthermore, prior studies have shown that higher GnPs concentrations can increase the matrix brittleness, reduce mechanical strength, and promote fatigue wear on surfaces [5, 25]. Figure 1 illustrates a schematic representation of the first stage of fabricating the tensile samples for the epoxy/GnPs matrix composites.

For the E/xGnPs matrix composites, the neat epoxy was prepared by mixing the resin and hardener in a 4:1 weight ratio, following the supplier's instructions. GnPs were added to the neat epoxy in specified weight fractions and mixed for two minutes at room temperature using an electric mixer to ensure uniform dispersion of GnPs nanoparticles within the epoxy matrix. The mixtures were blended at a low rotational speed of 250 rpm, minimizing both heat accumulation and bubble entrapment. Furthermore, the degassing process was performed at 50 °C for 30 minutes using a fixed vacuum of −70 kPa to ensure the removal of internal air bubbles from the mixtures. After degassing, the mixtures were poured into steel moulds to fabricate tensile test specimens for the E/xGnPs matrix composites, following the specifications of ASTM D638-99 [25]. The moulds were allowed to cure at ambient temperature for 24 hours, followed by a post-curing process at 100 °C for four hours, in accordance with the manufacturer's guidelines. The resulting tensile specimens had dimensions of 10 mm in thickness, 190 mm in total length, a gauge length of 80 mm, and a width of 10 mm.

In the second stage, flax/epoxy/GnPs (F/E/xGnPs) composites were fabricated with a constant flax fiber volume fraction of 25%, while the GnPs weight fraction − denoted by x − was varied across 0, 1.5, 3, 4.5, and 6 wt.%. Figure 2 illustrates a schematic representation of the second stage of fabricating the tensile and ILSS test samples for F/E/xGnPs composites. The fabrication process began with the preparation of flax fiber plies (220 × 300 mm). For each composite type, six-ply laminates were prepared and preheated at 60 °C for 30 minutes to eliminate moisture, following the supplier's recommendation. Simultaneously, the base matrices of E/xGnPs composites were prepared following the steps outlined in Stage 1 (steps 1–4), as shown in Figure 1.

The F/E/xGnPs composites were fabricated using the bridge-modified vacuum bagging technique. Fiber mats impregnated with resin were alternately stacked in the mold. A peel-ply layer was used to envelop the laminate stack, effectively controlling excess resin flow during the consolidation process. The laminate assembly was held under vacuum pressure of − 95 kPa for 24 hours at ambient temperature to cure, and subsequently post-cured at 100 °C for four hours. After curing, the composites were sectioned to prepare specimens for the ILSS and tensile testing. The ILSS samples were fabricated according to ASTM D2344, with dimensions of 20 mm in length, 10 mm in width, and a thickness of 3.0 ± 0.25 mm. For the tensile samples, the dimensions were 250 mm in length, 25 mm in width, and 3 ± 0.25 mm in thickness, as per ASTM D3039 [26].

Characterization of GnPs and the base-matrix E/xGnPs composites

The fourier transform infrared (FTIR), and Raman spectroscopy techniques were utilized to examine the chemical structure and assess possible interactions between the GnPs and the epoxy matrix in the E/xGnPs composites. The FTIR measurements were performed using a Nicolet

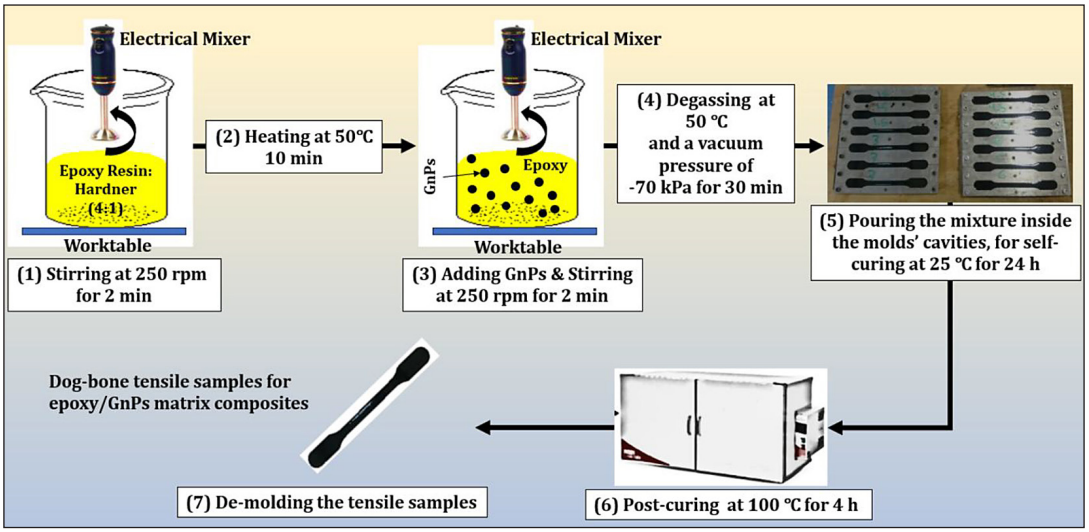

Figure 1. Schematic representation of stage 1: fabrication procedures of E/xGnPs base matrix composites

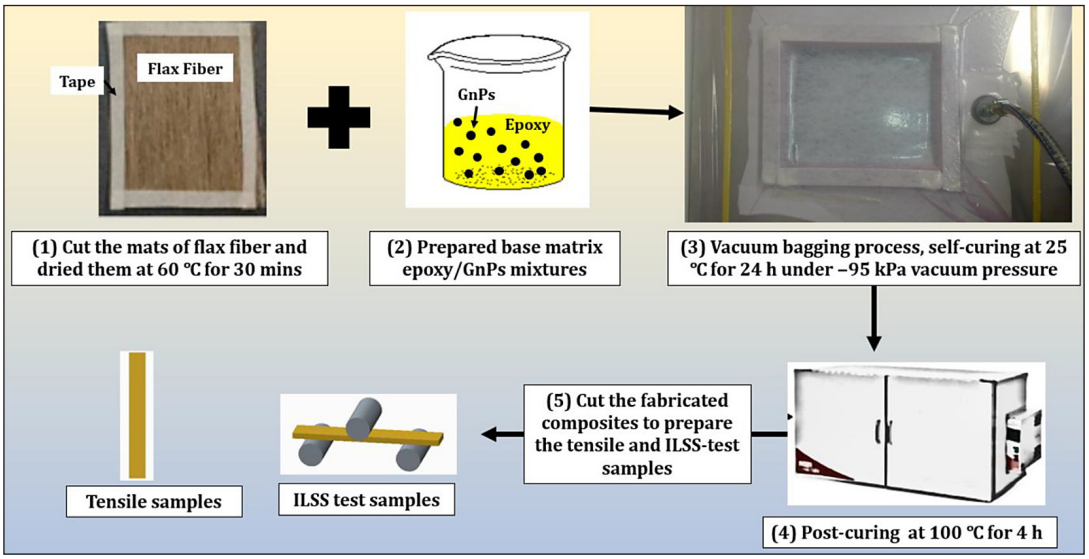

Figure 2. Schematic illustration for stage 2: fabrication procedures of F/E/xGnPs composites

iS50 FT-IR spectrometer. For analysis, samples – including GnPs, neat epoxy, and E/xGnPs composites – were ground into fine powders. The FTIR spectra were acquired using a Nicolet iS50 equipped with an ATR module, collecting 32 scans per sample within the spectral range of 500–4000 cm^{-1} at a resolution of 4 cm^{-1}.

The Raman spectra of both pristine GnPs powder and the E/xGnPs powders were recorded using a Renishaw inVia InSpect confocal Raman spectrometer. For the samples of the neat epoxy and E/xGnPs composites the laser power was 5% (1 mW) and for the GnPs was 1% (0.2 mW) was used. Spectra were collected between 500–3200 cm^{-1} with an acquisition time of 10 s.

Tensile, hardness and ILSS testing

Tensile tests were conducted to assess the mechanical properties – namely the fracture strength, stiffness, fracture strain, and toughness – of both the base E/xGnPs matrix composites and the F/E/xGnPs composites. Tensile testing was performed using an MTS 810 TestStar servo-hydraulic testing system (10 kN load capacity) with a crosshead speed of 1 mm/min. For the epoxy–GnPs matrix systems, testing procedures followed the ASTM D638-99 standard [25], while the tensile tests for the F/E/xGnPs composites followed ASTM D3039 [26]. For each composite type, three tensile specimens were tested, and the average results were recorded. Shore D hardness was measured

using a Type D durometer in accordance with ASTM D2240 [27], with five readings taken per sample to ensure measurement reliability.

The interlaminar shear strength between the flax fiber with different base-matrix E/xGnPs composites was evaluated using the short beam bending test, in accordance with ASTM D2344 [28]. Each sample measured 36 mm in length, 6 mm in width, and 3 mm in thickness. The testing was performed at a constant speed of 1 mm/min. To maintain a consistent span-to-thickness ratio, the support span was set at 12 mm. The diameters of the side support and the loading nose were 3 mm and 6 mm, respectively. For each composite, five samples were tested, and the average values were obtained. The values of ILSS were calculated based on the following equation:

$$ILSS = \frac{3P}{4(b*h)} \quad (1)$$

where: *ILSS* is the interlaminar shear strength (MPa), *P* is the maximum load (N), *b* is the sample's width (mm), and *h* is the sample's thickness (mm).

Scanning electron microscopy (SEM) analysis

The SEM analysis of the tensile and ILSS specimens from the F/E/xGnPs composites was carried out using a JEOL JCM-6000 Benchtop SEM. Imaging was conducted under a constant accelerating voltage of 5 kV. Before observation, the fracture surfaces were coated with a thin gold layer using a JEOL Smart Coater ion sputter system to improve the electrical conductivity and achieve clear, high-resolution images.

RESULTS AND DISCUSSION

Characterisation of GnPs and base-matrix of E/xGnPs composites

The FTIR spectral measurements were employed to identify the functional groups and examine the interactions between GnPs and epoxy in base matrix composites containing different GnPs weight fractions (1.5, 3, 4.5, and 6 wt.%). As shown in Figure 3, the FTIR spectrum of GnPs exhibits weak peaks near 1550 cm^{-1} and 1650 cm^{-1}, corresponding to C=O stretching of carboxylic groups and skeletal vibrations of graphitic carbon atoms, respectively. Pure epoxy displays characteristic peaks at 1604, 1505, 1454 cm^{-1} (C–C stretching in aromatic rings), 1298 cm^{-1} (asymmetric deformation of $–CH_2$), 1253, 1224 cm^{-1} (asymmetric C–O stretching of aromatic and aliphatic groups), 1032 cm^{-1} (symmetric aromatic C–O stretching), 826 cm^{-1} (–CH out-of-plane deformation in aromatic and epoxide rings), and 593 cm^{-1} (aromatic group frequencies), confirming successful polymerization of the resin.

In the E/GnPs base matrix composites, the FTIR spectra remain generally like that of neat epoxy, particularly at lower GnPs contents (1.5 and 3 wt.%). However, as the GnPs content increases to 4.5 and 6 wt.%, noticeable shifts in the main epoxy bands (by 5–15 cm^{-1}) are observed, suggesting an increase in the physical interactions between the GnPs and the epoxy matrix. These shifts, without the emergence of new peaks, indicate that the interactions are primarily non-covalent – likely Van der Waals forces and π–π stacking – rather than chemical bonding. Thus, the FTIR results confirm the formation of epoxy/GnPs composites and highlight how increasing GnPs content influences the interaction with the polymer matrix.

The Raman spectra shown in Figure 4 provide insight into the structural features of GnPs, neat epoxy, and E/xGnPs base-matrix composites. In Figure 4(a), the Raman spectrum of GnPs displays three prominent peaks: the D band at ~1310 cm^{-1} indicating the presence of structural defects, the G band at ~1580 cm^{-1} associated with in-plane vibrations of sp^2-bonded carbon atoms in the graphitic structure, and the G′ band (or 2D band) at ~2630 cm^{-1} characteristic of multilayer graphene. These peaks confirm the graphitic nature and defect structure of the GnPs.

Figure 4(b) shows the Raman spectra of neat epoxy and the base-matrix composites of epoxy/GnPs. Neat epoxy exhibits characteristic peaks at 653, 795, 1130, 1190, 1254, 1300, 1430, 1480, 1580, 2490, and 2880 cm^{-1}, corresponding to vibrational modes of the cured resin. Upon addition of GnPs, the composites show overlapping peaks from both epoxy and GnPs. Notably, the D and G bands of GnPs become more intense with increasing GnPs content, and the G and G′ bands shift slightly to lower wavenumbers. These changes indicate successful integration of GnPs into the epoxy matrix and suggest interfacial interactions, which can be used as confirmation of composite formation and GnPs dispersion.

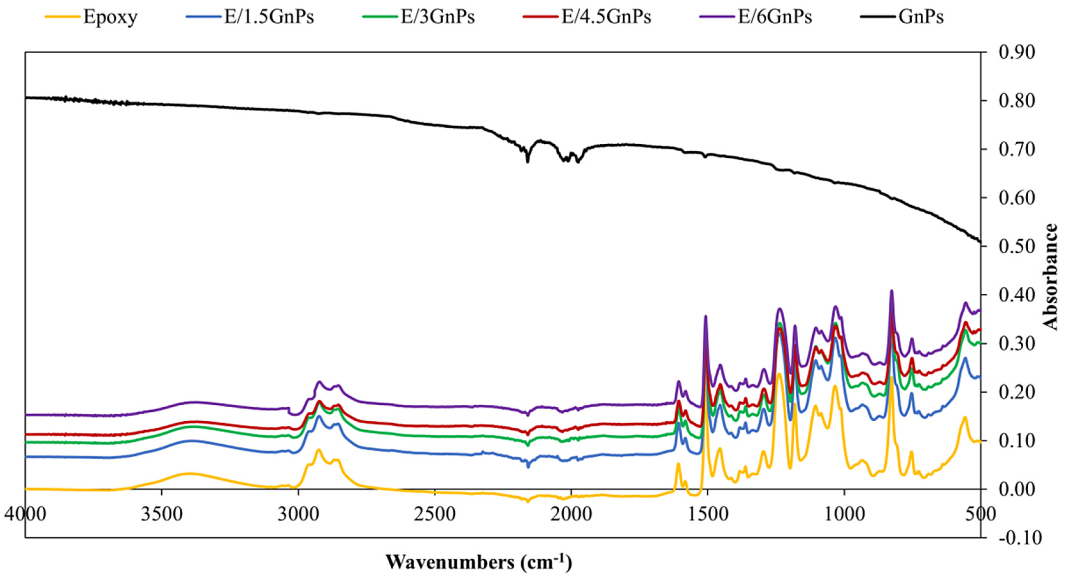

Figure 3. Spectral profiles from the FTIR spectra of GnPs, and base-matrix of E/xGnPs composites

Mechanical properties of base-matrix of E/xGnPs composites

The mechanical behaviour of the base matrix of epoxy/GnPs composites was characterized using tensile and Shore D hardness tests. This analysis provides essential insight into the role of GnPs content in modifying the matrix's performance and its interfacial bonding effectiveness with flax fibers in the reinforced composite system. Table 1 displays the mechanical properties of the base-matrix composites. The fracture strength of the neat epoxy was recorded at 59.91 ± 4.15 MPa, which is in good agreement with previously published works [23, 29, 30]. The addition of graphene nanoplatelets (GnPs) was found to progressively decrease the epoxy's fracture strength, strain at break, and overall toughness as their weight fraction is increased. For instance, the addition of 6 wt.% GnPs resulted in the highest reduction in fracture strength, fracture strain, and toughness, with decreases of 32.5%, 47.5%, and 68%, respectively, compared to the neat epoxy. Similar findings have been reported for various nanoparticles within polymer matrices, such as in epoxy/graphite composites [29]. The primary reason for this behaviour can be attributed to the agglomeration and aggregation phenomena of the nanoparticles. The tendency of nanoparticles to agglomerate increases with their concentration within the polymer matrix. Additionally, the viscosity of the polymer resin plays a significant role in this regard. However, in this study, to mitigate this issue, the mixing process was conducted at a temperature of 60 °C to reduce the viscosity of the epoxy resin, thereby minimizing the occurrence of such phenomena as much as possible.

On the other hand, the addition of GnPs led to an increase in the brittleness of the epoxy, as indicated by the rise in stiffness and hardness values. For example, the incorporation of 6 wt.% GnPs increased the stiffness and hardness of the epoxy by 22% and 13%, respectively. This behaviour can primarily be attributed to the inherent nature of GnPs as a brittle material. The GnPs used in this study have a stiffness value of 1000 GPa, which, combined with their high specific surface area-to-weight ratio, contributes to the observed increase in the brittleness properties.

Figure 5 displays SEM images of the tensile fracture surfaces observed in the neat epoxy and epoxy/GnPs composites with 1.5 wt.% and 6 wt.% GnPs loadings. The neat epoxy surface shows limited toughening characteristics, reflected in its relatively smooth, river-like morphology – ndicative of slight plastic deformation prior to failure. This observation corresponds with the higher fracture strain measured for the neat epoxy among all base matrix composites. In contrast, incorporating GnPs introduced clear alterations in the fracture surface characteristics. When increasing GnPs content, the fracture morphology becomes more brittle in appearance, marked by a diminished plastic deformation and a more fragmented surface structure, suggesting a reduction in the material's ductility. The squamous-like

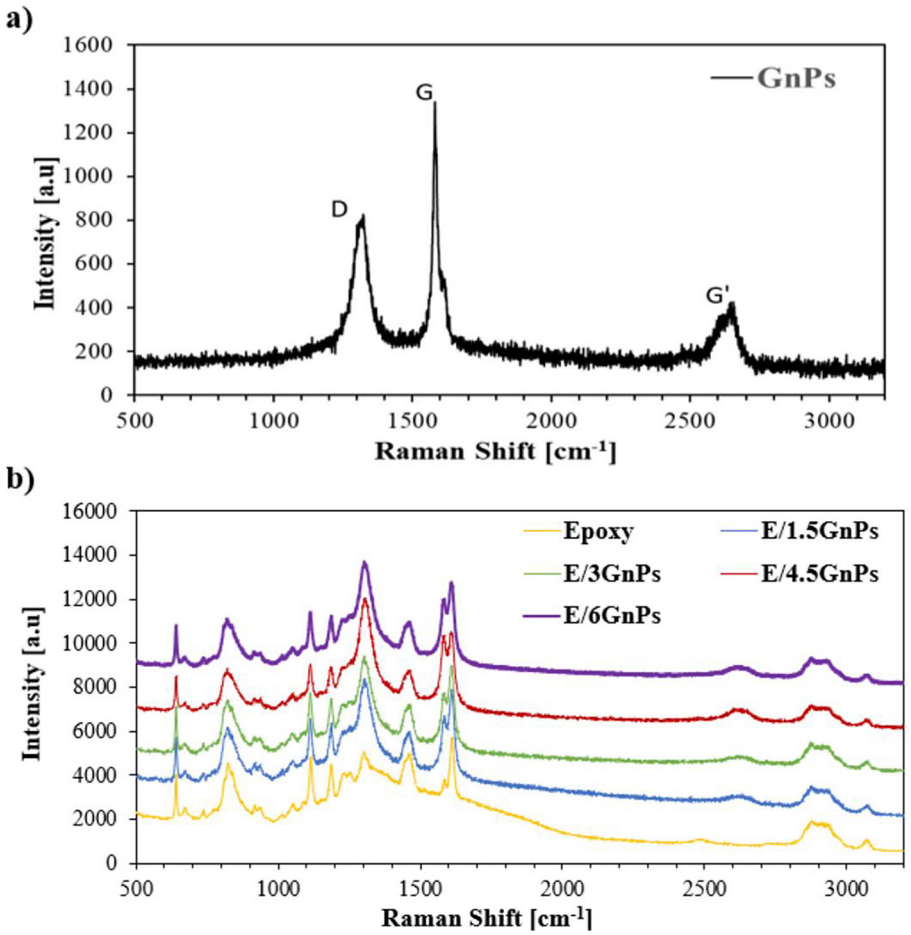

Figure 4. The Raman spectral analysis: (a) GnPs and (b) base-matrix of E/xGnPs composites

pattern became more pronounced and dominant with higher GnPs content, reflecting a more brittle fracture, which is consistent with our previous works [23, 29]. The decrease in fracture strain with increasing GnPs content, as displayed in Table 1, is consistent with these fracture features and further explains the observed changes. Also, the increase in the GnPs content led to an increase in the agglomeration of nanoparticles on GnPs inside the epoxy matrix as observed in Figure 5(c). The agglomeration and aggregation of nanoparticles act as stress concentrators, leading to a reduction in the strength of the composite. This phenomenon provides a clear explanation for the lowest fracture strength observed in the E/6GnPs composite, as shown in Table 1.

ILSS properties of F/E/GnPs composites

The influence of varying GnPs weight fractions in the epoxy resin on the bonding strength with flax fibers was assessed through ILSS measurements using the short-beam bending method. Figure 6 presents the trend in ILSS values for flax fiber-reinforced composites with varying GnPs contents. The results clearly show that the lower incorporation of GnPs, i.e., 1.5 wt.% of GnPs into the epoxy matrix results in the most significant improvement in ILSS value, with an improvement of approximately 18% compared to the neat epoxy resin. This improvement is mostly attributed to the high surface area of GnPs. The large surface area enhanced the mechanical interlocking – between the GnPs and the surrounding epoxy matrix. In addition, the fabrication process takes care to achieve a good dispersion of GnPs, resulting in more contact points at the interface and enabling an efficient load transfer between the matrix and fibers.

However, when the GnPs content exceeds 1.5 wt.% (e.g., 3, 4.5, and 6 wt.%), a gradual decline in ILSS is observed. For instance, the 6 wt.% of GnPs leads to a reduction in the ILSS value by 9% compared to neat epoxy. This reduction trend can be attributed to two main factors. Firstly, the inherent van der Waals forces between GnPs

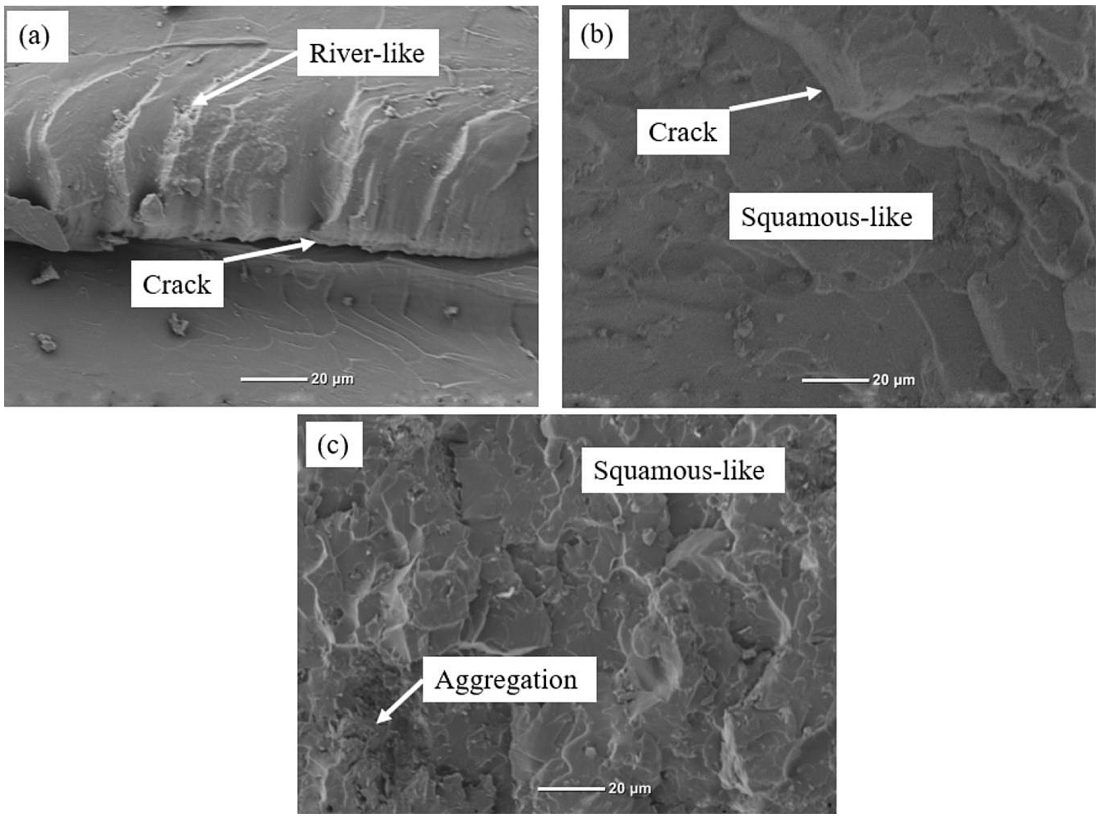

Figure 5. SEM images for fractured surfaces of the tensile samples of the base-matrix (E/xGnPs) composites: (a) the neat epoxy, (b) E/3GnPs and (c) E/6GnPs

Table 1. Mechanical properties of base-matrix (E/xGnPs) composites

Base-matrix composites	Fracture strength, (MPa)	Stiffness (GPa)	Fracture strain, %	Toughness ($MJ.m^{-3}$)	Shore D hardness
Epoxy	59.91 ± 4.15	1.10 ± 0.06	7.05 ± 1.69	2.67 ± 0.71	77.33 ± 2.05
E/1.5GnPs	50.79 ± 3.11	1.26 ± 0.02	4.64 ± 0.28	0.96 ± 0.10	80.67 ± 2.05
E/3GnPs	46.97 ± 2.20	1.33 ± 0.02	4.44 ± 0.37	0.92 ± 0.14	83.67 ± 2.05
E/4.5GnPs	46.07 ± 2.45	1.34 ± 0.01	4.34 ± 0.29	0.93 ± 0.16	85.00 ± 2.16
E/6GnPs	40.43 ± 2.20	1.34 ± 0.005	3.70 ± 0.20	0.85 ± 0.15	87.30 ± 1.65

sheets promote strong particle–particle attraction, leading to agglomeration and aggregation [31]. This dilemma becomes increasingly pronounced at higher weight fractions, as it disrupts the uniform distribution of nanoplatelets within the epoxy matrix. It is well established that such agglomeration and aggregation act as stress concentration zones, thereby inhibiting effective load transfer at the fiber–matrix interface [22, 24]. Second, higher GnPs loading significantly increases the viscosity of the epoxy resin, reducing its ability to thoroughly wet and impregnate the flax fibers. Poor wetting results in insufficient bonding and reduced interfacial adhesion [32]. Thus, while low GnPs content enhances the mechanical and interfacial performance of flax/epoxy composites, excessive GnPs loading adversely affects the composite due to dispersion challenges, viscosity-related processing difficulties, and interfacial inefficiencies.

The poor wetting of natural fiber's filaments is primarily associated with their inherent characteristics, in contrast to synthetic fibers, thereby complicating their compatibility with the polymer matrix in fiber-reinforced composites. For instance, Tian et al. [9] explored the influence of incorporating high silica nanoparticle loadings – up to 20 wt.% – on the interfacial bonding strength between carbon fibers and an epoxy matrix. The results demonstrated a consistent increase in ILSS values when rising the silica content. In the case of

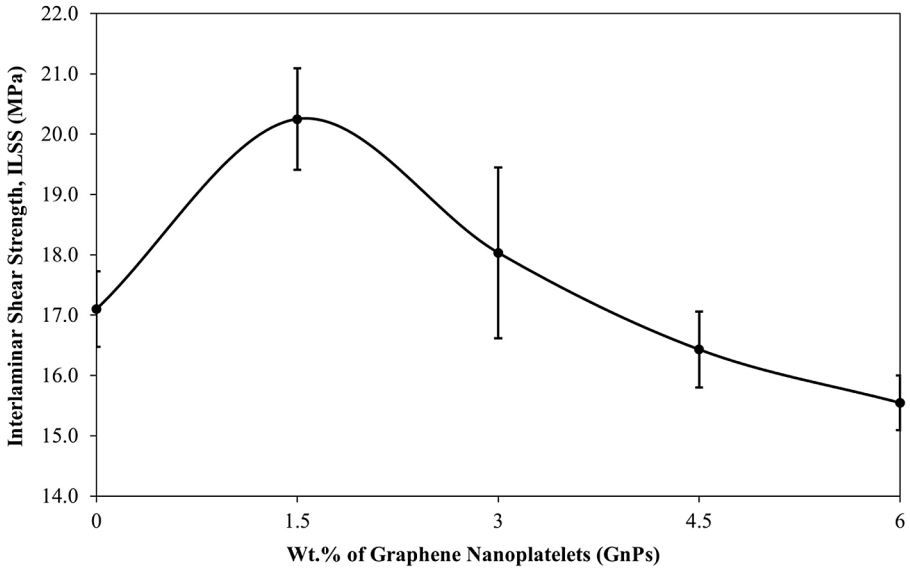

Figure 6. Interlaminar shear strength of flax/epoxy composites as a function of the inclusion amount of GnPs

synthetic fibers, a reduction in the ILSS at higher filler loadings is primarily attributed to the aggregation of nanoparticles within the polymer matrix. This reduction in the ILSS values beyond a weight fraction of 1.5 wt.% can be explained by both the aggregation and agglomeration of GnPs nanoparticles, as well as the poor wettability of flax fibers – resulting from the increased viscosity of the base matrix at higher nanoparticle loadings. The findings align well with the mechanical and tribological properties of the developed composites reported in our previous work [24], thereby offering additional insights into our earlier findings.

Figure 7 displays SEM images illustrating the level of interfacial cohesion at the flax/epoxy interface for the neat epoxy matrix, as well as for the E/1.5GnPs and E/6GnPs matrices, representing lower and higher GnPs contents, respectively. The SEM images revealed that both the neat epoxy resin and the E/1.5GnPs matrix exhibit a high level of interfacial cohesion, whereas the E/6GnPs matrix noticeably shows a reduced cohesion. This evidence highlights the negative impact of higher GnPs content on the viscosity of the epoxy matrix, which in turn, diminishes interfacial bonding. Ultimately, this reduction in cohesion weakens the bonding strength between the flax fibers and the epoxy matrix, thereby lowering the overall mechanical performance of the developed composites.

To mitigate this effect, additional processing measures could be considered – particularly at higher GnPs loadings – such as, increasing the processing temperature of the E/GnPs matrix. This would help to reduce the viscosity of the matrix mixture and improve the wetting of flax fiber filaments, thereby enhancing the interfacial adhesion and composite integrity.

Figure 8 displays SEM images of the ILSS samples for the F/E, F/E/1.5GnPs, and F/E/6GnPs composites. In Figure 8a, SEM analysis of the F/E composite reveals unencapsulated flax fibers, indicating a weak fiber–matrix interfacial bonding. In contrast, at 1.5 wt.% GnPs loading (Fig. 8b), the flax fibers are well encapsulated by the epoxy matrix, suggesting an improved wetting and enhanced interfacial cohesion. This improvement corresponds to a notable increase in the ILSS, as shown in Fig. 6, confirming the beneficial effect of uniformly dispersed GnPs at low concentrations. However, a further increase in the GnPs content beyond 1.5 wt.% results in a decline in the ILSS. As evident in Fig. 8c, nanoparticle agglomeration occurs at higher loadings, leading to inhomogeneous resin distribution and microstructural defects. These agglomerates act as stress concentrators and may serve as crack initiation sites under mechanical loading [22]. Additionally, the increased matrix viscosity at higher GnPs content can impair fiber wetting, further weakening the interfacial bond. As a result, the negative effects of nanoparticle aggregation and poor interfacial contact outweigh the reinforcing benefits of GnPs at excessive contents. These findings underscore the importance of optimizing nanofiller concentration to maintain strong fiber–matrix adhesion

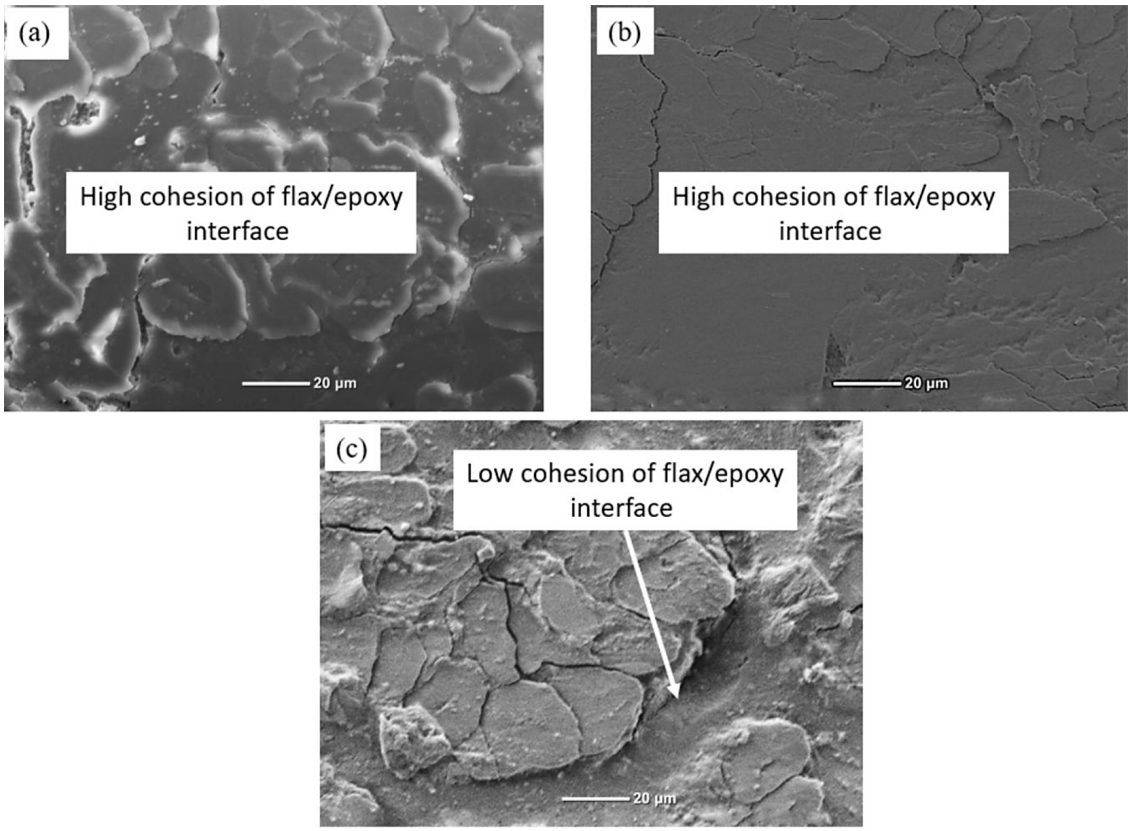

Figure 7. SEM images showing the level of interfacial cohesion at the flax/epoxy interface in the cases of: (a) F/E, (b) F/E/1.5GnPs, and (c) F/E/6GnPs composites

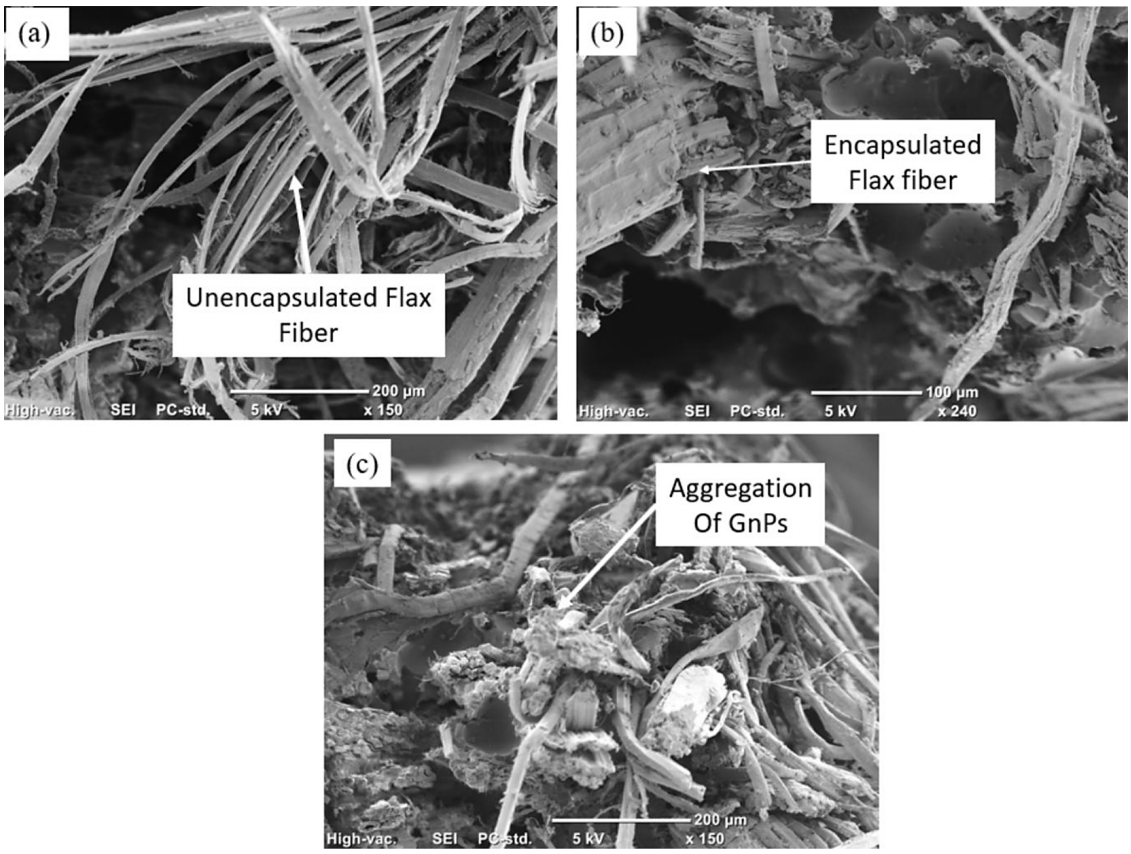

Figure 8. SEM images of the ILSS after testing for: (a) F/E, (b) F/E/1.5GnPs, and (c) F/E/6GnPs composites

and achieve high mechanical performance in natural fiber-reinforced epoxy composites**.**

Mechanical properties of F/E/GnPs composites

Figures 9–11 illustrate the mechanical properties of flax/epoxy/GnPs (F/E/GnPs) composites. For a more comprehensive analysis, the mechanical performance of each composite is compared to that of its corresponding epoxy/GnPs base matrix. It is important to note that, in many applications, the optimal weight fraction of nano-additives is governed by the specific performance requirements of the intended application. For example, our previous studies have reported that while higher nanoparticle content may be favourable for enhancing the lubrication properties of polymers, mechanical property improvements are typically achieved at lower filler loadings [23, 24, 29]. Therefore, such comparative analysis offers a more rational and contextually grounded interpretation of the results. FTIR and Raman characterisation analyses of the E/GnPs base matrix composites confirm a synergistic interaction between the GnPs and the epoxy matrix. As the GnPs utilized in this study are unfunctionalized, they lack the chemical reactivity necessary to modify the cross-linking density of the epoxy network, either by increasing or decreasing the proportion of the networked phase.

The hardness values of the F/E/xGnPs composites are presented in Figure 8. An increasing trend in composite hardness is observed with rising GnPs content, which is consistent with the trend noted in the E/GnPs matrix composites. The addition of flax fibers to the E/xGnPs composites appears to have a relatively minor impact on the hardness values. The primary reason for the increased hardness at higher GnPs content is the inherently brittle nature of GnPs, which possess a stiffness exceeding 1000 GPa [23]. Additionally, the high specific surface area of the GnPs – measured at 300 m^2/g in this study – enhances stress transfer at the filler–matrix interface, further contributing to the observed increase in hardness. Similar findings were reported on the epoxy/graphite [30] and PEEK/GnPs [33].

The fracture strength and modulus of elasticity of the F/E/GnPs composites are presented in Figures 10(a) and 10(b), respectively. The F/E composite exhibited the highest fracture strength, with a value of 139.53 ± 8.33 MPa. However, the fracture strength of the F/E/GnPs composites showed a decreasing trend with increasing GnPs content. For example, the F/E/1.5GnPs composite exhibited a marginal reduction of approximately 3%, whereas the F/E/6GnPs composite showed a significant decrease of 32% in fracture strength compared to the F/E composite. This behaviour is mainly attributed to the agglomeration and aggregation of GnPs within the epoxy matrix, which become more pronounced at higher filler concentrations [22, 24]. Additionally, the poor wetting of flax fiber filaments contributes to this reduction, as the increased GnPs content leads to a rise in the viscosity of the epoxy resin – thereby hindering effective fiber–matrix interaction [32], as previously discussed.

However, as mentioned earlier, absolute values of mechanical strength can sometimes be misleading; therefore, a more rational interpretation of the results can be achieved by comparing the mechanical performance of the F/E/GnPs composites relative to their corresponding matrix composites.

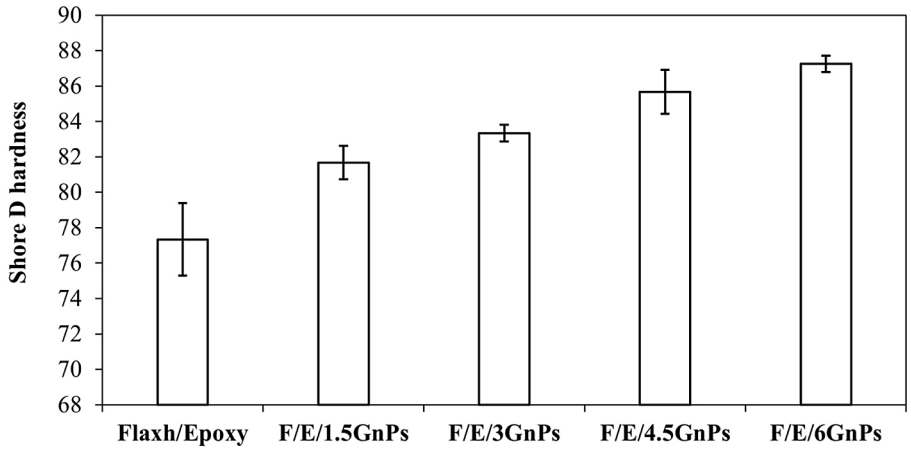

Figure 9. Shore D hardness values for Flax/Epoxy/GnPs composites

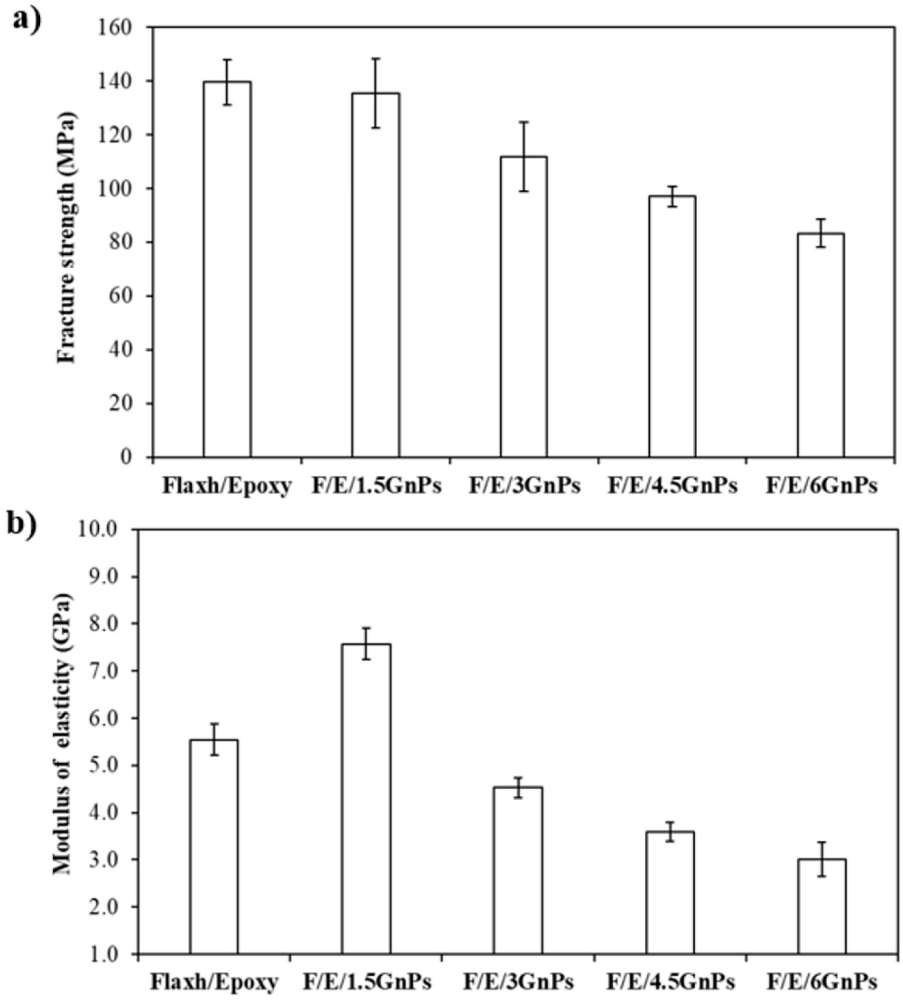

Figure 10. Mechanical properties of F/E/GnPs composites: (a) fracture strength and (b) modulus of elasticity

For instance, the fracture strength of the F/E, F/E/1.5GnPs, F/E/3GnPs, F/E/4.5GnPs, and F/E/6GnPs composites improved by 133%, 166%, 138%, 111%, and 106%, respectively, compared to their corresponding matrix composites – namely, neat epoxy, E/1.5GnPs, E/3GnPs, E/4.5GnPs, and E/6GnPs. These findings highlight the beneficial role of natural fiber reinforcement, even at higher nanoparticle loadings, despite the observed reduction in absolute strength. Interestingly, these improvement percentages closely align with the ILSS values presented in Figure 6. The maximum ILSS was recorded for the F/E/1.5GnPs composite, which also exhibited the highest improvement in fracture strength (166%) compared to its corresponding matrix composite, E/1.5GnPs. It is important to note that the addition of GnPs offers benefits beyond mechanical performance, enhancing properties such as thermal conductivity [34] and lubrication properties [23] to meet specific application requirements.

Overall, flax fiber has been shown to significantly enhance the mechanical performance of both neat epoxy and epoxy/GnPs-based matrices. Although the mechanical properties of natural fibers are inherently variable due to factors such as growth conditions, the tensile strength of flax fiber is commonly reported to be around 460 MPa [35]. Based on this value, the fiber contribution efficiency in F/E, F/E/1.5GnPs, F/E/3GnPs, F/E/4.5GnPs and F/E/6GnPs composites relative to their respective matrix bases is estimated at 87%, 88%, 74%, 65% and 57%, respectively. The incorporation of nanofillers is thought to enhance the effective interfacial area between the fibers and the matrix, thereby improving ILSS, especially at lower filler loadings. This may account for the notable improvement in mechanical strength observed with the incorporation of 1.5 wt.% GnPs.

The results for the modulus of elasticity, presented in Figure 10(b), indicate that the optimal

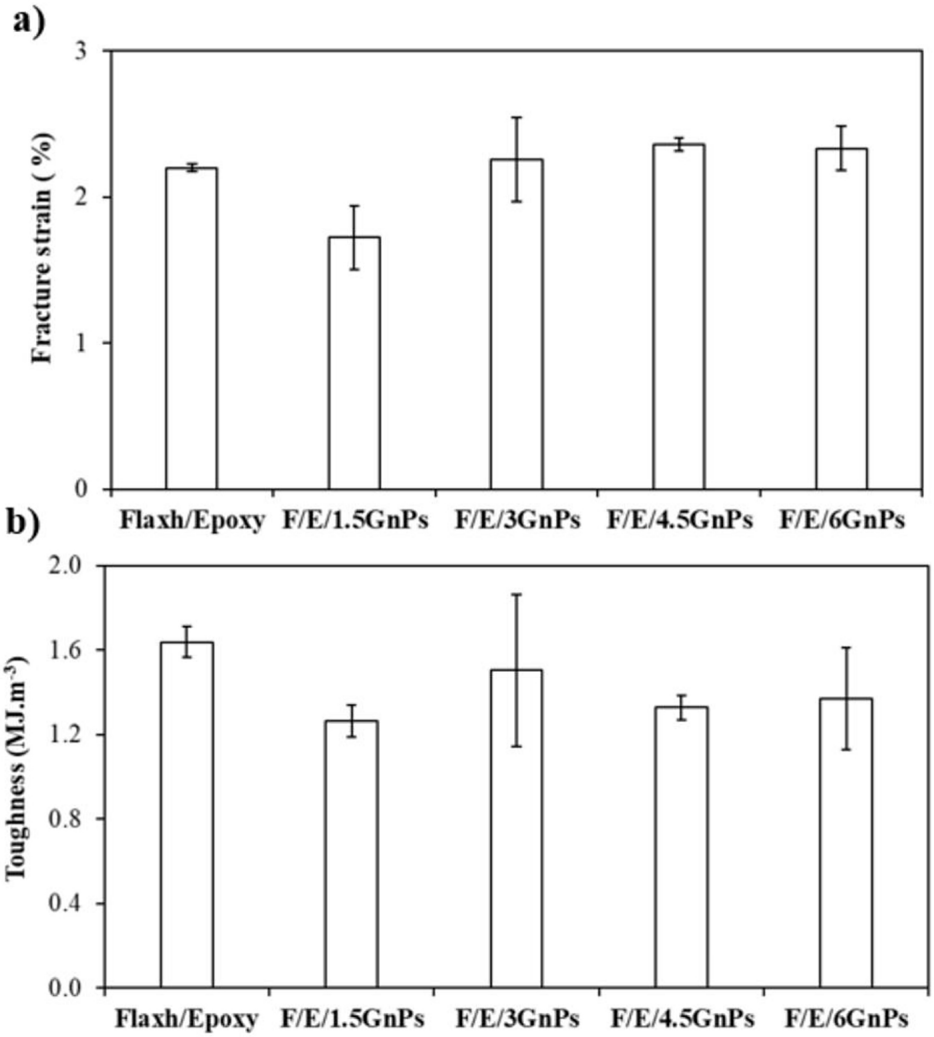

Figure 11. Mechanical properties of Flax/Epoxy/GnPs composites: (a) fracture strain and (b) toughness

GnPs content is 1.5 wt.%, corresponding to the F/E/1.5GnPs composite. This composite exhibited a 36% improvement over the F/E composite and a 500% increase relative to its corresponding matrix composite, E/1.5GnPs. This notable enhancement can be attributed to the uniform dispersion of GnPs at lower filler content, which facilitates effective stress transfer due to the high intrinsic stiffness of GnPs and improves interfacial bonding between the flax fibers and the matrix. In contrast, composites containing higher GnPs contents – specifically 3 wt%, 4.5 wt%, and 6 wt.% – showed a decline in modulus of elasticity compared to the F/E composite. This reduction is likely due to nanoparticle agglomeration, which becomes more pronounced at higher loadings. These agglomerates act as stress concentrators and hinder efficient load transfer. Moreover, the low interfacial cohesion observed at higher GnPs contents, as shown in Figure 7, provides additional support for this explanation.

The tensile strength and stiffness (modulus of elasticity) of the F/E/GnPs composite are compared in Table 2 with those of other NFRPs. Notably, the composite developed in this study demonstrated competitive mechanical performance, even with a relatively low flax fiber volume fraction of 25%, when compared to systems reinforced with other natural fibers such as bamboo, date palm, and kenaf. This performance is primarily attributed to the favourable mechanical properties of the commercially sourced flax fibers, which were pre-treated and supplied with uniform areal density – comparable to the consistency typically associated with synthetic fibers. Additionally, the modified mould design featuring a bridging element, as detailed in our previous work [24], may have contributed to the fabrication of laminates with a reduced density of manufacturing defects such as voids and air bubbles.

Table 2. Fracture strength (FS) and stiffness (E) of the F/E/GnPs composite in comparison with other NFRPs reported in the literature

Ref.	Material	*FS* (MPa)	*E* (GPa)	Improvement (%) in *TS* and *E*, respectively, compared with neat epoxy
Current study	Epoxy–25 V_r% flax fiber	139 ± 8.33	5.55 ± 0.6	132% and 400%
[30]	Epoxy–35 V_r% date palm fiber	67 ± 4.0	1.35 ± 0.16	22% and 111%
[36]	Epoxy–48 wt.% kenaf fiber	106.1 ± 2.5	10.7 ± 0.25	122% and 393%
[37]	Epoxy–42 V_r% bamboo fiber	222.7 ± 20	13.1 ± 2	181% and 424%

The fracture strain and stress–strain toughness values of the F/E/GnPs composites are presented in Figures 11(a) and 11(b), respectively. All F/E/GnPs composites exhibited a significant reduction in fracture strain compared to their corresponding base matrix composites (E/GnPs), indicating a decrease in ductility following flax fiber incorporation. This reduction can be attributed to the relatively low fracture strain of flax fibers – typically in the range of 1.5–1.8% [38] – which is lower than that of the E/GnPs base matrix composites, measured between 3.7% and 7%, as reported in Table 1. Consequently, the onset of fiber fracture occurs earlier in the loading process, limiting the composite's overall ability to sustain deformation. Furthermore, potential stress concentrations and interfacial debonding, particularly under conditions of increased matrix viscosity due to GnPs addition, may further restrict the strain capacity and reduce the energy absorption capability of the composite. This trade-off between strength and ductility should be carefully considered in applications where energy absorption or impact resistance is a critical performance requirement.

The toughness of the F/E composite is significantly reduced compared to its corresponding base matrix, neat epoxy. However, all F/E/xGnPs composites exhibited some improvement in toughness values relative to their respective base matrix composites, as reported in Table 1. This enhancement in toughness is likely due to the reinforcing effect of GnPs, which can contribute to crack-bridging and energy dissipation mechanisms within the matrix. Although the addition of flax fibers alone reduces toughness due to their lower fracture strain and the potential for interfacial debonding, the inclusion of GnPs may help arrest crack propagation and improve stress distribution – thereby enhancing the overall fracture resistance of the hybrid composites.

CONCLUSIONS

This study examined the influence of GnPs on the interfacial and mechanical properties of flax fiber-reinforced epoxy (F/E) composites. The optimal GnPs content was investigated on a range of 0–6 wt.% while maintaining a constant flax fiber volume fraction of 25%. Mechanical testing and interfacial analysis revealed that the incorporation of 1.5 wt.% GnPs provided the most favourable results. The F/E/1.5GnPs composite showed significant improvements, including a 166% increase in the fracture strength, a 500% increase in the modulus of elasticity compared to the E/1.5GnPs matrix, and an 18% improvement in the interlaminar shear strength (ILSS) compared to neat epoxy. These enhancements are attributed to the uniform GnPs dispersion, improved fiber–matrix adhesion, and more effective stress transfer. However, at higher GnPs loadings (≥ 3 wt.%), the mechanical performance was degraded due to nanoparticle agglomeration and increased matrix viscosity, which impaired fiber wetting and reduced interfacial cohesion. Although the addition of flax fibers slightly reduced the fracture strain and toughness, it substantially enhanced the strength and stiffness of the composites. SEM observations supported these findings, showing well-bonded interfaces at 1.5 wt.% GnPs and brittle fracture characteristics at higher contents. Overall, the results underscore the importance of optimising GnPs content to achieve a balanced performance in sustainable natural fiber-reinforced composite systems.

Acknowledgements

The authors gratefully acknowledge the support provided by the technicians and colleagues at the Centre for Future Materials (CFM), University of Southern Queensland (UniSQ), Australia.

REFERENCES

1. Boland CS, De Kleine R, Keoleian GA, Lee EC, Kim HC, Wallington TJ. Life cycle impacts of natural fiber composites for automotive applications: Effects of renewable energy content and lightweighting. Journal of Industrial Ecology 2016;20:179–89. https://doi.org/10.1111/jiec.12286
2. Slimani F, Ghanmi I, Ghanmi S, Guedri M. Contribution to manufactured a new thermoplastic biocomposite reinforced with natural fabric of date palm fibers without any treatment. Advances in Science and Technology Research Journal 2025;19:302–12. https://doi.org/10.12913/22998624/204232
3. Jaradat M, Duran JL, Murcia DH, Buechley L, Shen Y-L, Christodoulou C, Taha MR. Cognizant fiber-reinforced polymer composites incorporating seamlessly integrated sensing and computing circuitry. Polymers 2023;15:4401. https://doi.org/10.3390/polym15224401
4. Shuaib NA, Mativenga PT. Energy demand in mechanical recycling of glass fibre reinforced thermoset plastic composites. Journal of Cleaner Production 2016;120:198–206. https://doi.org/https://doi.org/10.1016/j.jclepro.2016.01.070
5. Akhshik M, Panthapulakkal S, Tjong J, Sain M. Life cycle assessment and cost analysis of hybrid fiber-reinforced engine beauty cover in comparison with glass fiber-reinforced counterpart. Environmental Impact Assessment Review 2017;65:111–7. https://doi.org/10.1016/j.eiar.2017.04.005.
6. Li X, Tabil LG, Panigrahi S. Chemical treatments of natural fiber for use in natural fiber-reinforced composites: A review. Journal of Polymers and the Environment 2007;15:25–33. https://doi.org/10.1007/s10924-006-0042-3
7. Yan L, Chouw N, Huang L, Kasal B. Effect of alkali treatment on microstructure and mechanical properties of coir fibres, coir fibre reinforced-polymer composites and reinforced-cementitious composites. Construction and Building Materials 2016;112:168–82. http://doi.org/10.1016/j.conbuildmat.2016.02.182
8. Kwon D-J, Shin P-S, Kim J-H, Baek Y-M, Park H-S, DeVries KL, Park J-M. Interfacial properties and thermal aging of glass fiber/epoxy composites reinforced with SiC and SiO_2 nanoparticles. Composites Part B: Engineering 2017;130:46–53. https://doi.org/10.1016/j.compositesb.2017.07.045
9. Tian Y, Zhang H, Zhang Z. Influence of nanoparticles on the interfacial properties of fiber-reinforced-epoxy composites. Composites Part A: Applied Science and Manufacturing 2017;98:1–8. https://doi.org/10.1016/j.compositesa.2017.03.007
10. Asim M, Jawaid M, Abdan K, Ishak MR. Effect of alkali and silane treatments on mechanical and fibre-matrix bond strength of kenaf and pineapple leaf fibres. Journal of Bionic Engineering 2016;13:426–35. https://doi.org/http://dx.doi.org/10.1016/S1672-6529(16)60315-3
11. Fiore V, Scalici T, Nicoletti F, Vitale G, Prestipino M, Valenza A. A new eco-friendly chemical treatment of natural fibres: Effect of sodium bicarbonate on properties of sisal fibre and its epoxy composites. Composites Part B: Engineering 2016;85:150–60. https://doi.org/10.1016/j.compositesb.2015.09.028
12. le Duigou A, Bourmaud A, Balnois E, Davies P, Baley C. Improving the interfacial properties between flax fibres and PLLA by a water fibre treatment and drying cycle. Industrial Crops and Products 2012;39:31–9. https://doi.org/10.1016/j.indcrop.2012.02.001
13. Seki Y, Sarikanat M, Sever K, Erden S, Ali Gulec H. Effect of the low and radio frequency oxygen plasma treatment of jute fiber on mechanical properties of jute fiber/polyester composite. Fibers and Polymers 2010;11:1159–64. https://doi.org/10.1007/s12221-010-1159-5
14. Ragoubi M, George B, Molina S, Bienaimé D, Merlin A, Hiver J-M, Dahoun A. Effect of corona discharge treatment on mechanical and thermal properties of composites based on miscanthus fibres and polylactic acid or polypropylene matrix. Composites Part A: Applied Science and Manufacturing 2012;43:675–85. https://doi.org/10.1016/j.compositesa.2011.12.025
15. Torres FG, Cubillas ML. Study of the interfacial properties of natural fibre reinforced polyethylene. Polymer Testing 2005;24:694–8. https://doi.org/10.1016/j.polymertesting.2005.05.004
16. Tang Y, Ye L, Zhang D, Deng S. Characterization of transverse tensile, interlaminar shear and interlaminate fracture in CF/EP laminates with 10 wt% and 20 wt% silica nanoparticles in matrix resins. Composites Part A: Applied Science and Manufacturing 2011;42:1943–50. https://doi.org/http://dx.doi.org/10.1016/j.compositesa.2011.08.019
17. Ahmadi-Moghadam B, Taheri F. Influence of graphene nanoplatelets on modes I, II and III interlaminar fracture toughness of fiber-reinforced polymer composites. Engineering Fracture Mechanics 2015;143:97–107. https://doi.org/10.1016/j.engfracmech.2015.06.026
18. Hsieh T-H, Chen W-J, Chiang C-L, Shen M-Y. Environmental aging effect on interlaminar properties of graphene nanoplatelets reinforced epoxy/carbon fiber composite laminates. Journal of Reinforced Plastics and Composites 2018;37:1177–90. https://doi.org/10.1177/0731684416637219
19. Awan FS, Fakhar MA, Khan LA, Subhani T. Study of interfacial properties of carbon fiber epoxy matrix composites containing graphene nanoplatelets.

Fibers and Polymers 2019;20:633–41. https://doi.org/10.1007/s12221-019-8596-6

20. Yao X, Gao X, Jiang J, Xu C, Deng C, Wang J. Comparison of carbon nanotubes and graphene oxide coated carbon fiber for improving the interfacial properties of carbon fiber/epoxy composites. Composites Part B: Engineering 2018;132:170–7. https://doi.org/10.1016/j.compositesb.2017.09.012
21. Yuan X, Zhu B, Cai X, Qiao K, Zhao S, Yu J. Influence of different surface treatments on the interfacial adhesion of graphene oxide/carbon fiber/epoxy composites. Applied Surface Science 2018;458:996–1005. https://doi.org/10.1016/j.apsusc.2018.06.161
22. Dang C-Y, Shen X-J, Nie H-J, Yang S, Shen J-X, Yang X-H, Fu S-Y. Enhanced interlaminar shear strength of ramie fiber/polypropylene composites by optimal combination of graphene oxide size and content. Composites Part B: Engineering 2019;168:488–95. https://doi.org/10.1016/j.compositesb.2019.03.080
23. Eayal Awwad KY, Yousif BF, Fallahnezhad K, Saleh K, Zeng X. Influence of graphene nanoplatelets on mechanical properties and adhesive wear performance of epoxy-based composites. Friction 2021;9:856–75. https://doi.org/10.1007/s40544-020-0453-5
24. Awwad KE, Yousif B, Mostafa A, Alajarmeh O, Zeng X. Tribological and mechanical performances of newly developed eco-epoxy composites incorporating flax fibres and graphene nanoplatelets. Journal of Reinforced Plastics and Composites 2022:073168442211434. https://doi.org/10.1177/07316844221143451
25. ASTM D638-99. Standard test method for tensile properties of plastics. American Society for Testing Materials 2000.
26. ASTM. D3039/D3039M. Annual Book of ASTM Standards 2014.
27. ASTM D2240. Standard Test Method for Rubber Property. American Society for Testing Materials n.d.
28. ASTM D2344. Standard Test Method for Short-Beam Strength of Polymer Matrix Composite Materials and Their Laminates n.d.
29. Eayal Awwad KY. Effects of adding graphite to epoxy resin on its mechanical properties and mild-to-severe wear performance at its heat distortion temperature. Tribology in Industry 2024;46:298–314. https://doi.org/10.24874/ti.1552.09.23.01
30. Shalwan A, Yousif BF. Influence of date palm fibre and graphite filler on mechanical and wear characteristics of epoxy composites. Materials & Design 2014;59:264–73. https://doi.org/http://dx.doi.org/10.1016/j.matdes.2014.02.066
31. Atif R, Inam F. Reasons and remedies for the agglomeration of multilayered graphene and carbon nanotubes in polymers. Beilstein Journal of Nanotechnology 2016;7:1174–96. https://doi.org/10.3762/bjnano.7.109
32. Moudood A, Rahman A, Öchsner A, Islam M, Francucci G. Flax fiber and its composites: An overview of water and moisture absorption impact on their performance. Journal of Reinforced Plastics and Composites 2019;38:323–39. https://doi.org/10.1177/0731684418818893
33. Puértolas JA, Castro M, Morris JA, Ríos R, Ansón-Casaos A. Tribological and mechanical properties of graphene nanoplatelet/PEEK composites. Carbon 2019;141:107–22. https://doi.org/10.1016/j.carbon.2018.09.036
34. Jarosinski L, Rybak A, Gaska K, Kmita G, Porebska R, Kapusta C. Enhanced thermal conductivity of graphene nanoplatelets epoxy composites. Materials Science- Poland 2017;35:382–9. https://doi.org/10.1515/msp-2017-0028
35. Wang H, Xian G, Li H. Grafting of nano-TiO_2 onto flax fibers and the enhancement of the mechanical properties of the flax fiber and flax fiber/epoxy composite. Composites Part A: Applied Science and Manufacturing 2015;76:172–80. https://doi.org/10.1016/j.compositesa.2015.05.027
36. Fiore V, Di Bella G, Valenza A. The effect of alkaline treatment on mechanical properties of kenaf fibers and their epoxy composites. Composites Part B: Engineering 2015;68:14–21. https://doi.org/10.1016/j.compositesb.2014.08.025
37. Huang J-K, Young W-B. The mechanical, hygral, and interfacial strength of continuous bamboo fiber reinforced epoxy composites. Composites Part B: Engineering 2019;166:272–83. https://doi.org/10.1016/j.compositesb.2018.12.013
38. Bogoeva-Gaceva G, Avella M, Malinconico M, Buzarovska A, Grozdanov A, Gentile G, Errico ME. Natural fiber eco-composites. Polymer Composites 2007;28:98–107. https://doi.org/10.1002/pc.20270